



Supplement of

Occurrence and source apportionment of perfluoroalkyl acids (PFAAs) in the atmosphere in China

Deming Han et al.

Correspondence to: Jinping Cheng (jpcheng@sjtu.edu.cn)

The copyright of individual parts of the supplement might differ from the CC BY 4.0 License.

Supplementary material

CONTENT

Table S1. Physical and chemical properties of target PFAAs compounds.....	2
Table S2. The geographic information and annual temperature in different sampling sites of atmospheric PFAAs....	3
Table S3. MS parameters, MDLs, LODs, LOQs values and recovery rates for individual compounds of PFAAs.....	5
Table S4. The measured abundances of PFAAs in this study (n=268)	7
Table S5. Correlation analysis of PFAAs in the atmosphere in China.....	8
Figure S1. Spatial distributions of 23 sampling sites of atmospheric PFAAs in China	9
Figure S2. Temporal variations of PFAAs concentrations in selected four typical sites.....	10
Figure S3. The spatial distributions of fluoride related products manufacturers in China.....	11
Figure S4. The spatial distributions of fluoride related products manufacturers in Zhejiang site	12
Figure S5. The backward trajectories of air mass extracted by Hysplit trajectory model.....	14
Section S1. Sampling rate of XAD–PAS in this investigation.....	15
Section S2. PMF analysis and uncertainty assessment.....	16
Reference.....	18

NINETEEN pages: FIVE tables and FIVE figures, TWO sections,.

Table S1. Physical and chemical properties of target PFAAs compounds

Component	Abbreviation	Molecular structure	Molecular weight	Bio-concentration factor ^a	logK _{ow} ^b	P _L (mmHg) ^c
Perfluoroalkane carboxylic acids (PFCAs)						
Perfluoropentanoic acid	PFPeA	C4F9COOH	263.98	1.00	5.29	7.9±0.4
Perfluorohexanoic acid	PFHxA	C5F11COOH	313.98	1.00	5.97	3.1±0.5
Perfluoroheptanoic acid	PFHpA	C6F13COOH	363.97	1.00	6.86	0.5±0.6
Perfluorooctanoic acid	PFOA	C7F15COOH	413.97	1.90	7.75	0.3±0.7
Perfluorononanoic acid	PFNA	C8F17COOH	463.97	11.26	8.64	0.2±0.8
Perfluorodecanoic acid	PFDA	C9F19COOH	513.96	44.30	9.53	0.0±0.9
Perfluoroundecanoic acid	PFUdA	C10F21COOH	563.96	128.19	10.42	0.0±0.9
Perfluorododecanoic acid	PFDoA	C11F23COOH	613.95	235.68	11.31	0.0±1.0
Perfluorotridecanoic acid	PFTTrDA	C12F25COOH	663.95	474.19	12.19	0.0±1.1
Perfluorotetradecanoic acid	PFTeDA	C13F27COOH	713.95	1903.40	13.08	0.0±1.2
Perfluoroalkane sulfonic acids (PFSAs)						
Perfluorobutane sulfonic acid	PFBS	C4F9SO3H	299.98	1.00	3.68	/ ^d
Perfluorohexane sulfonic acid	PFHxS	C6F13SO3H	399.97	1.00	5.25	/
Perfluorooctane sulfonic acid	PFOS	C8F17SO3H	499.97	1.00	7.03	/

^a: Predicted data are generated using the Advanced Chemistry Development, Inc. (Canada), cited from (Yu, Liu et al. 2018);

^b: Predicted octanol–water partitioning coefficients from individual PFAAs structure, cited from (Buck, Franklin et al. 2011, Yu, Liu et al. 2018);

^c: Predicted pure compound vapor pressure, unit of mmHg at 298 K, cited from (Buck, Franklin et al. 2011, Yu, Liu et al. 2018);

^d: “/” means lack of related data.

1 **Table S2. The geographic information and annual temperature in different sampling sites of atmospheric PFAAs**

I.D.	Region	Province	Type	Location	Elevati on (m)	Monthly temperature (°C) ^a	mean	Gross Product (10 ⁸ RMB) ^b	Domestic Resident population (10 ⁴) ^b	Crude (10 ⁴ tons) ^b	plastic
1	Northern	of Beijing	Urban	Haidian District	31	−5 – 24		127.75	2171	28014.94	
2	China, NC	Tianjin	Urban	Jinnan District	3.3	−4 – 25		332.42	1557	18549.19	
3		Shanxi	Rural	Linshui County, Jincheng city	376	−11 – 17		79.47	3702	15528.42	
4	Eastern	of Shanghai	Urban	Minhang District	4.5	5 – 28		364.04	2418	30632.99	
5	China, EC	Zhejiang	Rural	Yinzhou District, Ningbo City	4	4 – 23		896.29	5657	51768.26	
6		Jiangsu	Urban	Changzhou City	5	2 – 26		1175.39	8209	85869.76	
7		Anhui	Urban	Yinquan District, Fuyang City	30	2 – 27		137.35	6225	27018	
8		Fujian	Urban	Huian Country, Quanzhou City	30	12 – 26		235.74	3911	32182.09	
10		Jiangxi	Urban	Jiujiang City	32.2	4 – 26		25.46	4622	20006.31	
9		Shandong	Urban	Laishan District, Yantai City	47	−1 – 24		710.42	10006	72634.15	
11	Southern	of Guangdong	Urban	Nanshan District, Shenzhen City	7	15 – 26		695.31	11169	89705.26	

12	China, SC	Hainan	Urban	Meilan District, Haikou City	12	18 – 26	19.67	926	4462.54
13	Central	of Hubei	Urban	Yunxi District, Shiyan City	437	1 – 24	191.86	5902	35478.09
14	China , CC	Henan	Urban	Gaoxin District, Zhenzhou City	110	–2 – 26	232.47	9559	44552.83
15		Hunan	Urban	Huaxin District, Hengyang City	103	7 – 27	48.4	6860	33902.96
16	Northwestern of	Xinjiang	Urban	Tacheng City	427	–14 – 18	621.72	2445	10881.96
17	China, NW	Shaanxi	Urban	Beilin District, Xi'an City	397	–1 – 24	478.63	3835	21898.81
18		Gansu	Urban	Chengguang District, Lanzhou City	1517	–7 – 19	121.57	2626	7459.9
19	Southwestern of	Sichuan	Urban	Shuangliu District, Chengdu City	506	4 – 23	214.94	3789	15901.68
20	China, SW	Yunnan	Urban	Lanchang Country, Puer City	1950	3 – 19	319.76	4369	23409.24
21		Guizhou	Urban	Xinren Country, Qiandongnan City	1379	6 – 22	127.75	2171	28014.94
22	Northeastern of	Heilongjiang	Urban	Beilin District, Suihua City	172	–22 – 19	332.42	1557	18549.19
23	China, NE	Liaoning	Rural	Neizhou Country, Huludao City	118	–12 – 21	79.47	3702	15528.42

2 ^a: Meteorological data originated from China Meteorological Administration, <http://www.cma.gov.cn/>;

3 ^b: Data originated from China Statistic Yearbook 2018, National Bureau of Statistics China, <http://www.stats.gov.cn/tjsj/ndsj/>;

Table S3. MS parameters, MDLs, LODs, LOQs values, recovery rates and blank values for individual compounds of PFAAs

Analogues	Parent	Daughter	Declustering	Collision	Retention	MDLs	LODs	LOQs	Recovery	Filed bank	Laboratory	Internal Standards
	ions (m/z)	ion (m/z)	potential (V) ^a	energy (eV) ^b	time (s)	(pg/m ³)	(pg/m ³)	(pg/m ³)	rate (%)	(pg/m ³)	blank (pg/m ³)	
PFCAs												
PFPeA	263	219	-40	-34	3.16	0.41	0.31	1.05	96±17	0.41±0.14	0.22±0.17	1,2- ¹³ C ₂ -PFHxA
PFHxA	313	269	-35	-36	3.42	0.18	0.14	0.47	108±22	0.48±0.06	0.37±0.39	1,2- ¹³ C ₂ -PFHxA
PFHpA	363	319→169	-55	-28	3.70	0.22	0.16	0.55	93±16	0.62±0.07	0.22±0.32	1,2,3,4- ¹³ C ₄ -PFOA
PFOA	413	369→169	-45	-39	3.99	0.33	0.26	0.87	91±13	0.93±0.11	0.41±0.29	1,2,3,4- ¹³ C ₄ -PFOA
PFNA	463	419→219	-40	-44	4.32	0.61	0.46	1.53	89±17	0.57±0.20	0.20±0.25	1,2,3,4,5- ¹³ C ₅ -PFNA
PFDA	513	469→219	-50	-47	4.67	0.56	0.42	1.39	93±11	0.35±0.19	0.28±0.22	1,2- ¹³ C ₂ -PFDA
PFUdA	563	519→269	-45	-61	5.02	0.28	0.21	0.70	88±16	0.31±0.09	0.31±0.13	1,2- ¹³ C ₂ -PFUdA
PFDoA	613	569→169	-45	-65	5.35	0.28	0.21	0.70	94±18	0.44±0.09	0.15±0.18	1,2- ¹³ C ₂ -PFDoA
PFTTrDA	663	619→169	-50	-59	5.64	0.34	0.26	0.87	102±17	0.09±0.11	0.05±0.11	1,2- ¹³ C ₂ -PFDoA
PFTeDA	713	669→169	-65	-57	5.94	0.14	0.31	1.03	97±21	0.12±0.14	0.06±0.13	1,2- ¹³ C ₂ -PFDoA
PFSAAs												

PFBS	299	80→99	-45	-64	3.19	0.25	0.20	0.66	81±25	0.11±0.08	0.27±0.46	¹⁸ O ₂ -PFHxS
PFHxS	399	80→99	-55	-87	3.70	0.16	0.12	0.40	86±13	0.16±0.05	0.42±0.27	¹⁸ O ₂ -PFHxS
PFOS	499	80→99	-55	-98	4.31	0.24	0.19	0.63	95±15	0.75±0.08	0.54±0.61	1,2,3,4- ¹³ C ₄ -PFOS
Internal Standards												
1,2- ¹³ C ₂ -PFHxA	315	270	-75	-41	3.40	/	/	/	/	/	/	/
1,2,3,4- ¹³ C ₄ -PFOA	417	372	-40	-41	3.99	/	/	/	/	/	/	/
1,2,3,4,5- ¹³ C ₅ -PFNA	468	423	-84	-52	4.34	/	/	/	/	/	/	/
1,2- ¹³ C ₂ -PFDA	515	470	-87	-51	4.69	/	/	/	/	/	/	/
1,2- ¹³ C ₂ -PFUdA	565	520	-79	-61	5.02	/	/	/	/	/	/	/
1,2- ¹³ C ₂ -PFDoA	615	570	-66	-55	5.35	/	/	/	/	/	/	/
¹⁸ O ₂ -PFHxS	403	103	-55	97	3.72	/	/	/	/	/	/	/
1,2,3,4- ¹³ C ₄ -PFOS	503	80	-80	97	4.31	/	/	/	/	/	/	/

^a: cited from Karásková et al., 2018.

^b: cited from Karásková et al., 2018 and Liu et al., 2015.

Table S4. The measured abundances of PFAAs in this study (n=268)

Analogues	Detection	Average value	Standard deviation	Minimum value	Maximum value	Median value
	frequency (%)	(pg/m ³)	(pg/m ³)	(pg/m ³)	(pg/m ³)	(pg/m ³)
PFCAs						
PFPeA	84.8	4.96	4.77	BDL	35.2	3.55
PFHxA	92.1	5.36	7.17	BDL	79.7	3.73
PFHpA	94.7	3.42	3.71	BDL	28.9	2.39
PFOA	100	8.19	8.03	0.36	70.4	6.24
PFNA	96.6	3.07	2.77	BDL	22.7	2.52
PFDA	96.2	4.13	3.74	BDL	30.5	3.36
PFUdA	75.6	1.24	1.32	BDL	6.72	0.86
PFDoA	63.5	0.56	0.50	BDL	3.18	0.45
PFTTrDA	37.3	0.58	0.56	BDL	3.57	0.47
PFTeDA	41.7	0.19	0.25	BDL	2.25	0.11
PFSAAs						
PFBS	62.2	1.96	1.85	BDL	9.39	1.37
PFHxS	71.6	0.99	1.38	BDL	13.2	0.56
PFOS	100	5.20	4.30	0.34	25.5	3.87

BDL: below detection limit.

Table S5. Correlation analysis of PFAAs in the atmosphere in China

	PFPeA	PFHxA	PFHpA	PFOA	PFNA	PFDA	PFUdA	PFDoA	PFTTrDA	PFTeDA	PFBS	PFHxS
PFHxA	0.70**											
PFHpA	0.12	0.31*										
PFOA	0.69**	0.77**	0.68**									
PFNA	0.66**	0.66**	0.65**	0.70**								
PFDA	0.54**	0.67**	0.72**	0.84**	0.61**							
PFUdA	0.16	0.32	0.15	0.2	0.14	0.23						
PFDoA	0.39*	0.33	0.27	0.38	0.31	0.32	0.61**					
PFTTrDA	0.53*	0.48**	0.3	0.42	0.44	0.51**	0.65**	0.62**				
PFTeDA	0.21	0.4	0.39*	0.36*	0.27	0.39	0.72**	0.59**	0.79**			
PFBS	0.68**	0.26	0.15	0.26	0.15	0.39	0.14	0.23	0.28	0.18		
PFHxS	0.57*	0.69**	0.27	0.42*	0.57**	0.64**	0.3	0.43*	0.54*	0.38*	0.28	
PFOS	0.69**	0.42*	0.32	0.33	0.36	0.37*	0.25	0.41*	0.46*	0.38	0.63**	0.40*

*: represent $p < 0.05$;

** : represent $p < 0.01$.

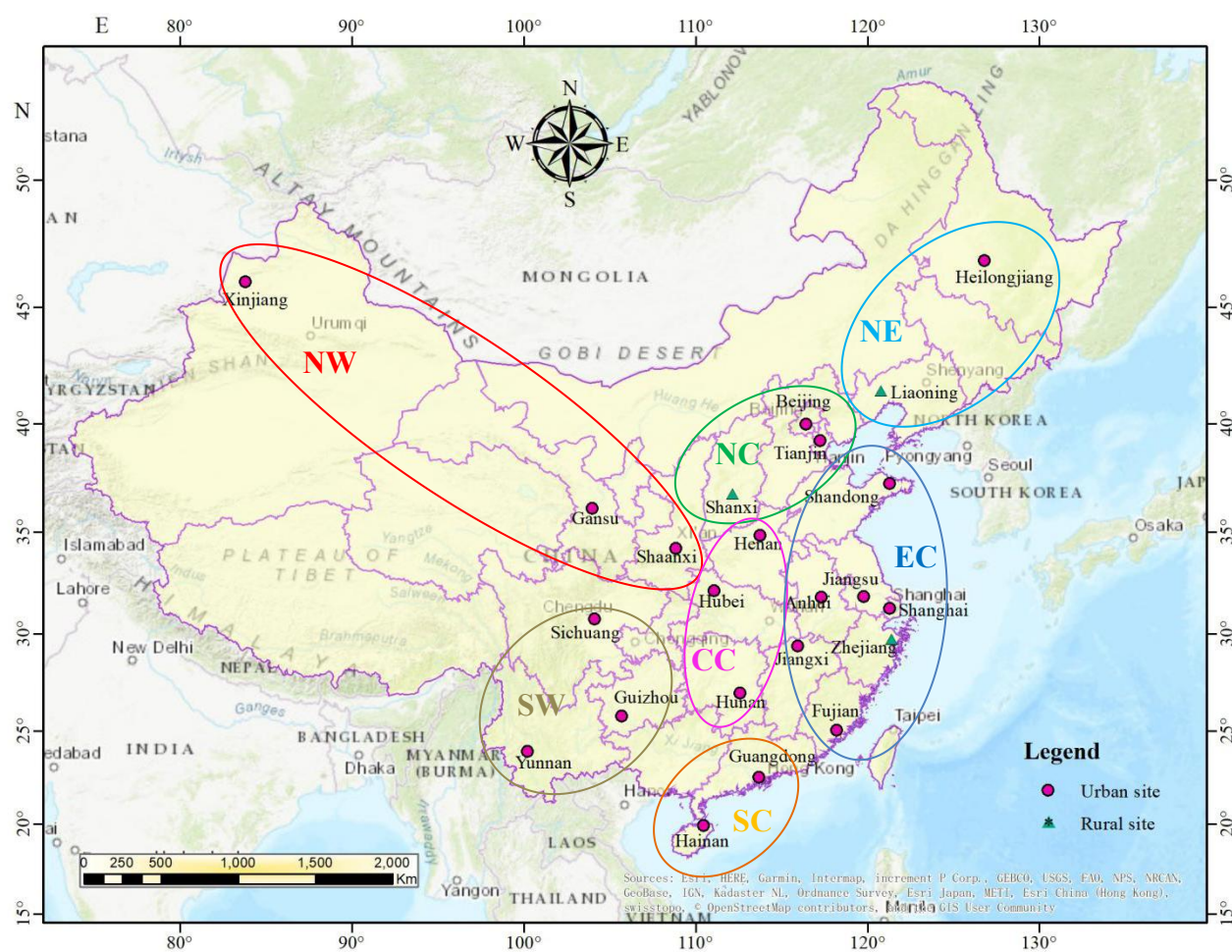


Figure S1. Spatial distributions of 23 sampling sites of atmospheric PFAAs in China (including 20 urban sites, red circles; and three rural site, green triangles).

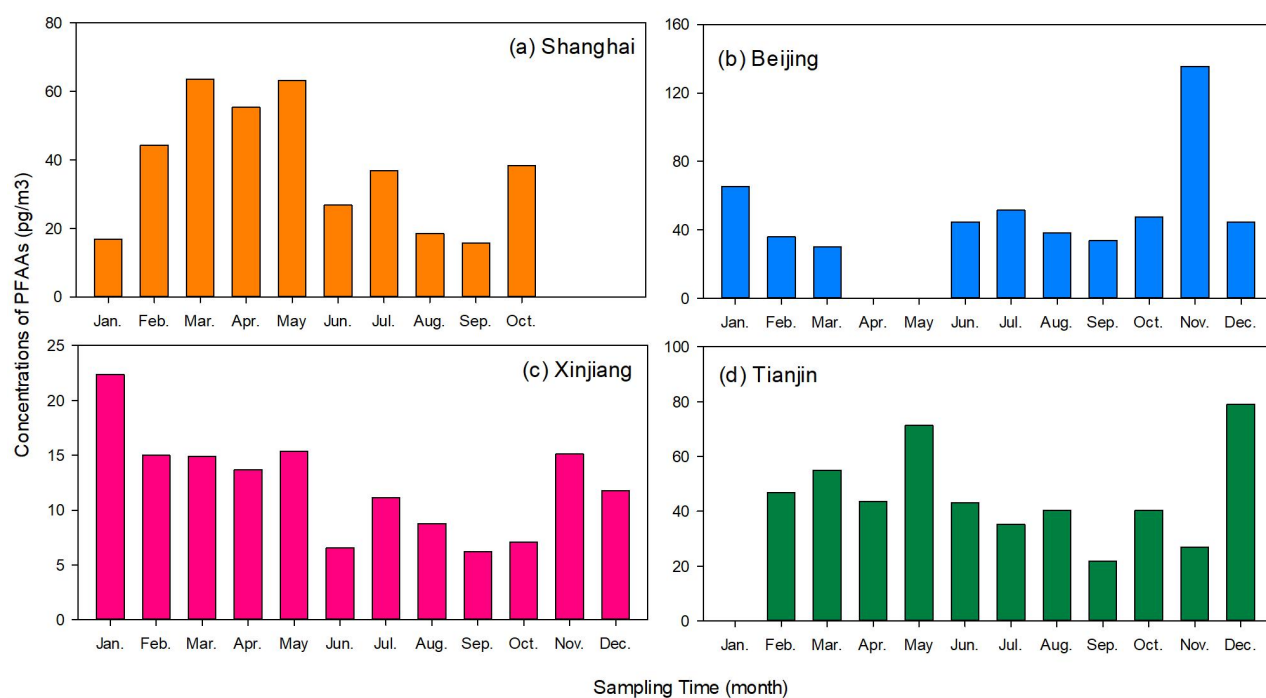


Figure S2. Temporal variations of PFAAs concentrations in selected four typical sites: Shanghai, Beijing, Xinjiang and Tianjin.

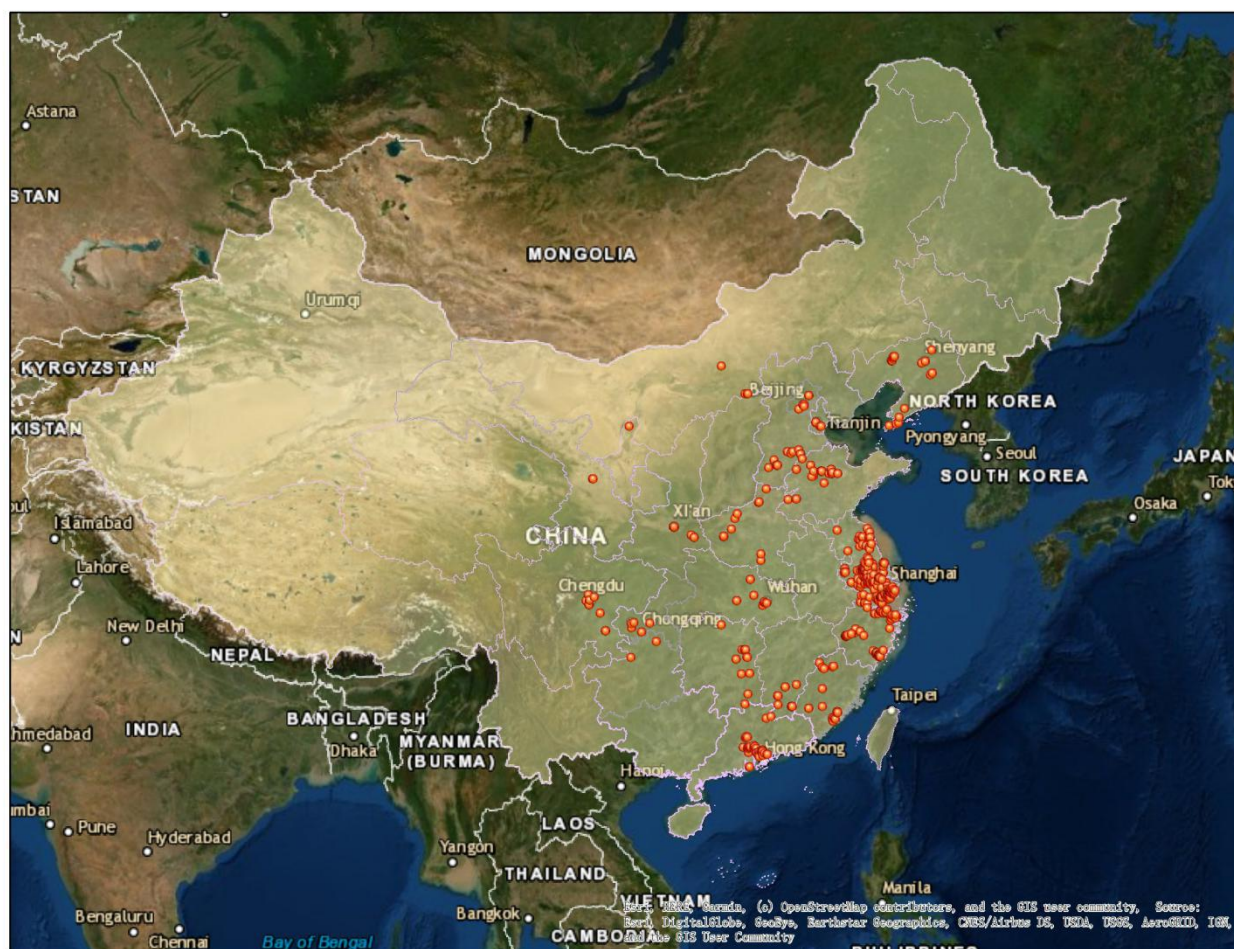


Figure S3. The spatial distributions of fluoride related products manufacturers in China and the different geographical conditions (note that the fluoride related manufacturers including textiles, crude plastic, paint coating, packaging materials, while part of fluoride related industries were not included in this figure)

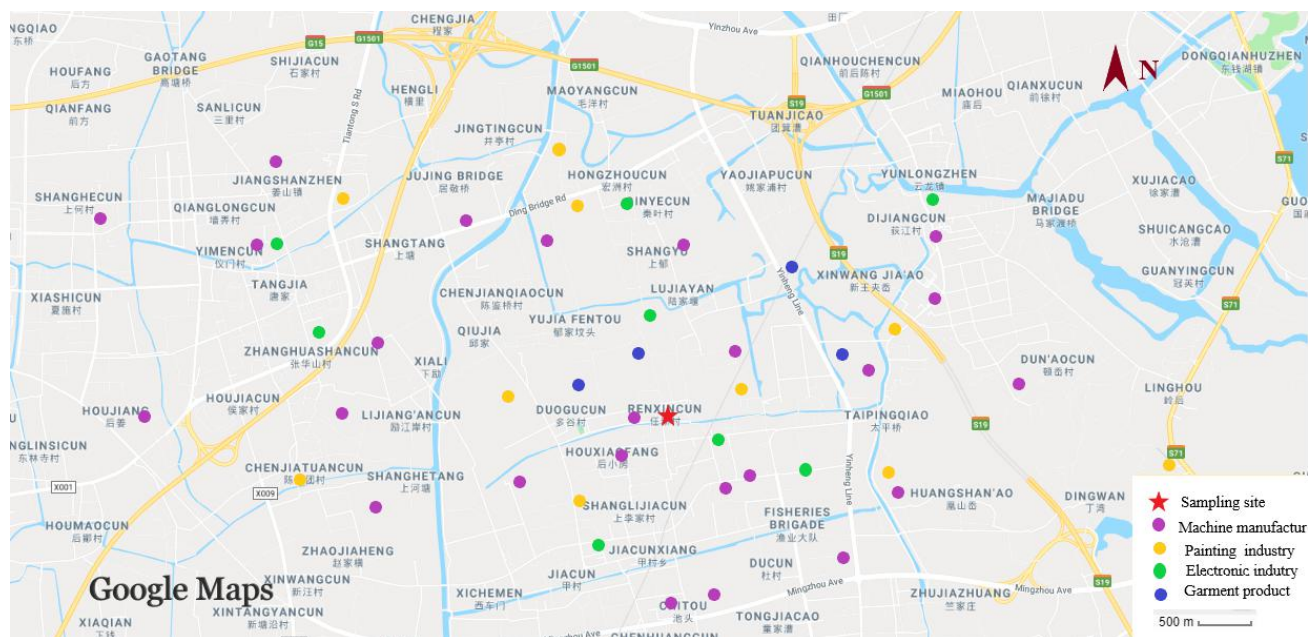
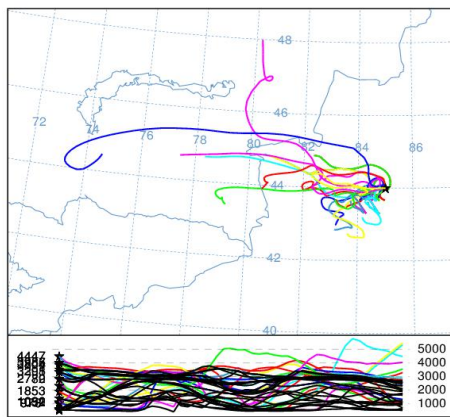
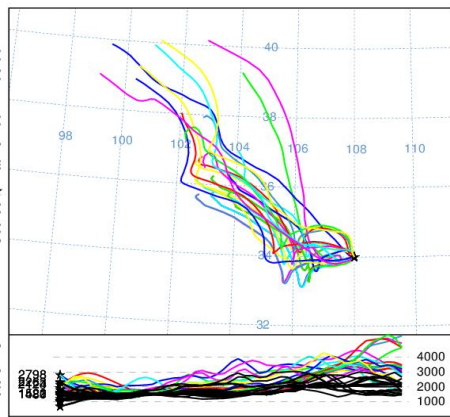


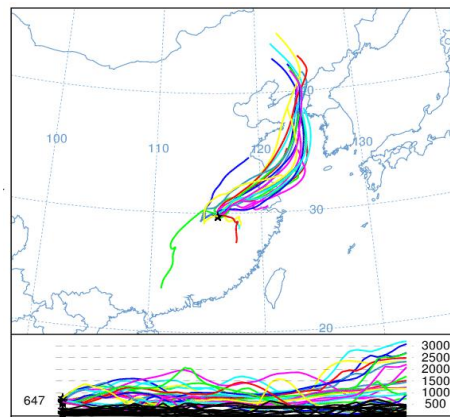
Figure S4. The spatial distributions of fluoride related products manufacturers in Zhejiang site (a small village in Ningbo City)



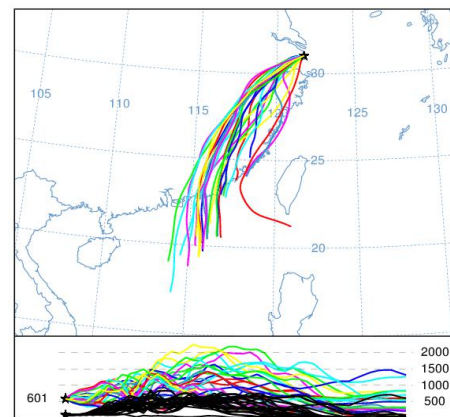
Tacheng, Xinjiang; Summer



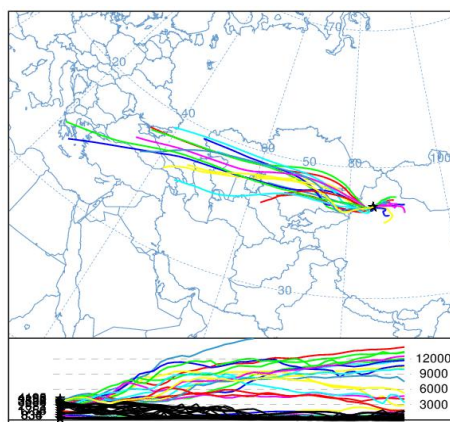
Xi'an, Shaanxi; Summer



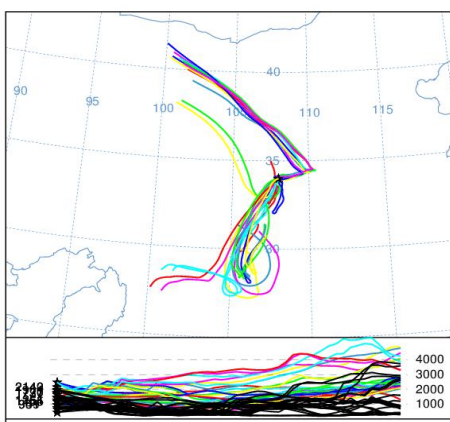
Jiujiang, Jiangxi; Summer



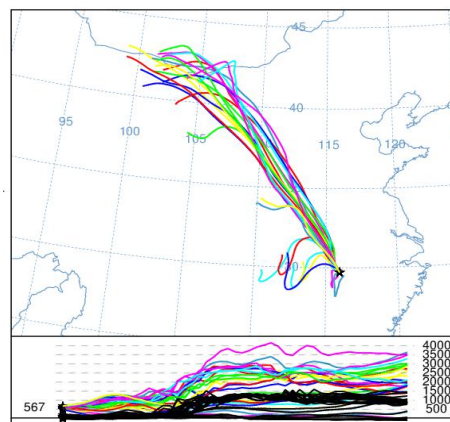
Shanghai; Summer



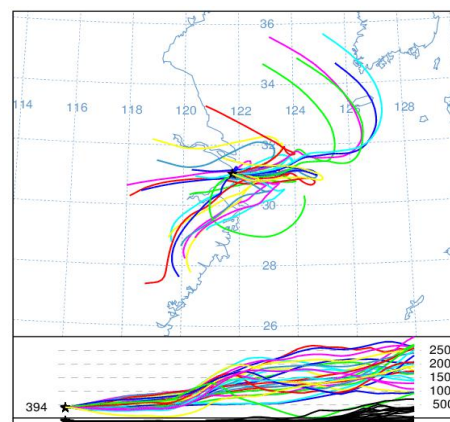
Tacheng, Xinjiang; Winter



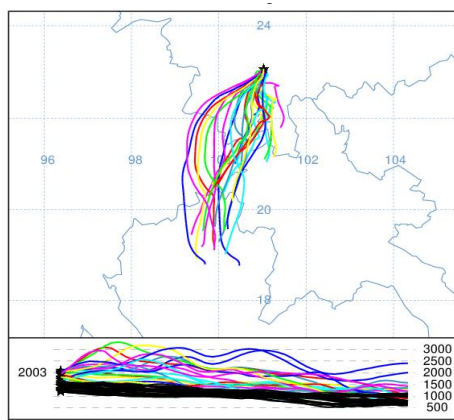
Xi'an, Shaanxi; Winter



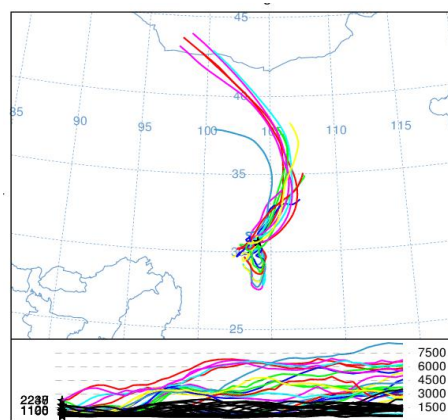
Jiujiang, Jiangxi; Winter



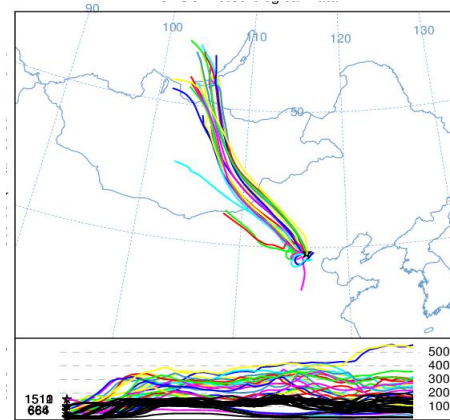
Shanghai; Winter



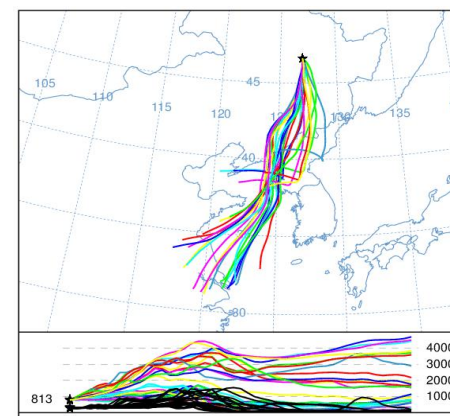
Pu'er, Yunnan; Summer



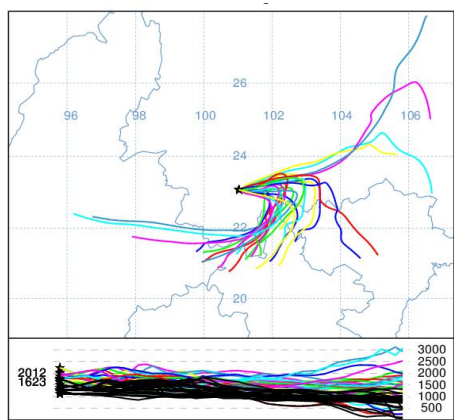
Chengdu, Sichuan; Summer



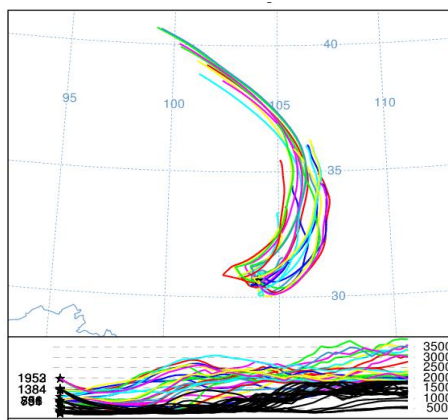
Beijing; Summer



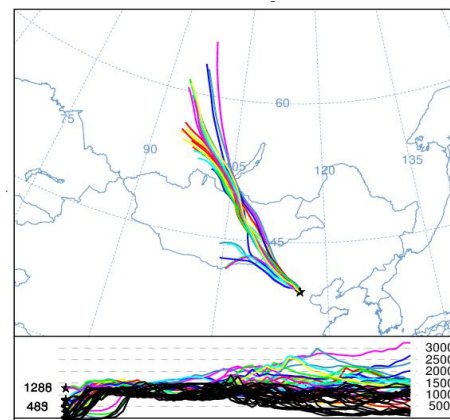
Suihua, Heilongjiang; Summer



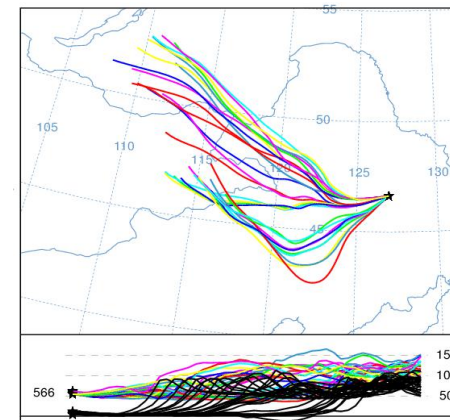
Pu'er, Yunnan; Winter



Chengdu, Sichuan; Winter



Beijing; Winter



Suihua, Heilongjiang; Winter

Figure S5. The backward trajectories of air mass extracted by Hysplit trajectory model

Section S1. Sampling rate of XAD–PAS in this investigation

Sampling rate of XAD–PAS is a crucial factor to derive air concentrations from the amounts of chemicals accumulated in the XAD resin. Previous literature suggested the sampling rate of XAD–PAS of 3.5–4.5 m³/d for PFASs (Li, Vento et al. 2011, Liu, Zhang et al. 2015, Tian, Yao et al. 2018). However, the actual sampling rate is dynamically variable, and affected by several factors. In this study, a standard solution containing mass labeled 1,2,3,4-¹³C₄–PFOA and 1,2,3,4-¹³C₄–PFOS (20 ng/mL) was spiked directly onto the upper XAD resin in the Shanghai sampling site (Floor of 5–story building of School of Environmental Science and Engineering in Shanghai Jiao Tong University) for one month in April 2017, to account for analyte losses during sampling. The sampling rate was calculated as flowing formulas:

$$R = -\ln(C_t/C_0) \times d \times A \times (K_{XAD}/t) = -\ln(C_t/C_0) \times V \times (K_{XAD}/t) \quad (S1)$$

$$\log K_{XAD} = 0.6366 \times \log(K_{OW} \times S_W/S_A) \quad (S2)$$

$$S_A = P_L/(RT) \quad (S3)$$

where C_t/C_0 represents the measured recoveries of 1,2,3,4-¹³C₄–PFOA and 1,2,3,4-¹³C₄–PFOS; V represents absorbent volume, 207.7(cm³); K_{XAD} represent ¹³C₈–PFOA partition coefficient between air and XAD; t represents sampling time, 30 d; K_{OW} , S_W , and S_A , represent octanol–air partition coefficient (6.3), water solubility, and air solubility, respectively; P_L and R represent liquid vapor pressure and gas constant (8.314 J/(mol·K)), respectively. The $\log P_L$, and $\log S_W$ values was set as 1.3(Pa), and 0.24 (mg/L) in the present study.

The sampling rate of XAD–PAS was calculated as 3.2 m³/d in the selected geographical site. However, higher temperature and wind speed were suggested to have positive effect on sampler uptake efficiency, while negative effect on the sorption capacity. Although the sampling rate of PFAAs were proposed of site-specific under different meteorological conditions, we have not conduct the depuration compounds loss test in all the 23 sampling sites. Since our calculated XAD–PAS rate value was very close to the recommended rate of 3.5–4.5 m³/d for PFAAs, the rate value of 3.2 m³/d was used in the present study.

Section S2. PMF analysis and uncertainty assessment

Positive matrix factorization (PMF) is considered an advanced algorithm among various receptor models, which has been successfully applied for source identification of environmental pollutants (Han, Fu et al. 2018; Han Fu et al. 2019). PMF has the following advantages: each data point is given an uncertainty-weighting; the factors in PMF are not necessarily orthogonal to each other and there is no non-negativity constraint with PMF. In the present study, PMF 5.0 (US EPA) was used to apportion the contributions of different sources to PFAAs in the atmosphere. The matrix X represents an ambient data set in which i represents the number of samples and j the number of chemical species. The goal of multivariate receptor modeling is to identify sources (p), the species profile (f) of each source and the amount of mass (g) contributed by each source to each individual sample as well as the residuals (e_{ij}), as following equation:

$$X_{ij} = \sum_{k=1}^p g_{ik} f_{kj} + e_{ij} \quad (S1)$$

The PMF solution minimizes the objective function Q based on these uncertainties (u):

$$Q = \sum_{i=1}^n \sum_{j=1}^m \left[\frac{X_{ij} - \sum_{k=1}^p g_{ik} f_{kj}}{u_{ij}} \right]^2 \quad (S2)$$

The input data files of PMF consist of concentrations and uncertainty matrices, and the uncertainty data were calculated as Equation (S3) as suggested by PMF User Guide. The missing values were represented by average values, while measurements below MDL (method detection limit) were replaced by two times of the corresponding MDL values. The “weak” variables were down-weighted, while “bad” variables were omitted from the analysis process.

$$\begin{cases} \text{Unc}_i = \frac{5}{6} \times \text{MDL}_i & C_i \leq \text{MDL}_i \\ \text{Unc}_i = \sqrt{(C_i \times \text{Error Fraction})^2 + \left(\frac{1}{2} \times \text{MDL}_i\right)^2} & C_i > \text{MDL}_i \end{cases} \quad (S3)$$

The model was run 20 times with 49 random seeds to determine the stability of goodness-of-fit values. If the number of sources is estimated properly, the theoretical Q value should be approximately the number of degrees of freedom or the total number of data points. Three to six factors were examined, and four factors were found to be the most appropriate

and most reasonably interpretable. Q (True) is the goodness-of-fit parameter calculated including all points, while Q (Robust) is the goodness-of-fit parameter calculated excluding points not fit by the model, Q (Robust) and Q (True) were 21672.9 and 25935, respectively, with $Q(\text{true})/Q_{\text{exp}}$ value of 12.56. Additionally, approximately 97% of the residuals calculated by PMF were within the range of -3 to 3 , indicating a good fit of simulated results. The factor did not show oblique edges, suggesting there were little rotation for the solution. All these features implied the model simulation result was acceptable.

Reference

- Buck, R. C., et al. (2011). "Perfluoroalkyl and polyfluoroalkyl substances in the environment: terminology, classification, and origins." *Integr Environ Assess Manag* **7**(4): 513–541.
- Han, D., et al. (2018). "Non-polar organic compounds in autumn and winter aerosols in a typical city of eastern China: size distribution and impact of gas-particle partitioning on PM_{2.5} source apportionment." *Atmos. Chem. Phys.* **18**(13): 9375–9391.
- Han D , et al. (2019). "Investigate the impact of local iron-steel industrial emission on atmospheric mercury concentration in Yangtze River Delta, China." *Environmental Science Pollution and Research.* **26**(6): 5862–5872.
- Karášková, P. et al. (2018). A critical assessment of passive air samplers for per- and polyfluoroalkyl substances, *Atmos. Environ.*, 185, 186-195.
- Li, J., et al. (2011). "Perfluorinated Compounds in the Asian Atmosphere." *Environmental Science & Technology* **45**(17): 7241.
- Liu, B., et al. (2015). "Perfluorinated compounds (PFCs) in the atmosphere of Shenzhen, China: Spatial distribution, sources and health risk assessment." *Chemosphere* **138**: 511–518.
- Tian, Y., et al. (2018). "Occurrence and Phase Distribution of Neutral and Ionizable Per- and Polyfluoroalkyl Substances (PFASs) in the Atmosphere and Plant Leaves around Landfills: A Case Study in Tianjin,China." *Environmental Science & Technology* **52**(3): 1301.
- Yu, S., et al. (2018). "Characteristics of perfluoroalkyl acids in atmospheric PM₁₀ from the coastal cities of the Bohai and Yellow Seas, Northern China." *Environmental Pollution* **243**: 1894–1903.
- Hu, X. C., et al. (2016). "Detection of Poly- and Perfluoroalkyl Substances (PFASs)in U.S. Drinking Water Linked to Industrial Sites, Military Fire TrainingAreas, and Wastewater Treatment Plants." *Environ Sci Technol Lett* **3**(10):

344-350.